

# SOLAR AIR CONDITIONING SYSTEMS WITH PCM SOLAR COLLECTORS

L. H. Alva S., J. E. González\*, and N. Dukhan

University of Puerto Rico-Mayagüez  
Department of Mechanical Engineering  
Mayagüez, Puerto Rico, 00681-9045

## ABSTRACT

This paper investigates the technical feasibility of using a compact, air-cooled, solar absorption air conditioning system coupled to an innovative array of solar collectors. The absorption system is single-effect with lithium bromide and water as the absorbent and refrigerant fluid pair. The geographical location of interest is Puerto Rico and similar subtropical regions. The heat input to the absorption system generator is provided by an array of novel flat plate solar collectors that integrate the thermal storage. The proposed collectors have a phase change material (PCM) integrated into them as the storage mechanism. The PCM-integrated solar collector eliminates the need of conventional storage tanks, thus reducing cost and space. The present work uses a paraffin-graphite composite as the PCM to increase the conductivity of the PCM matrix. The paraffin's melting point is around 89°C which is appropriate for use in single-effect absorption systems. The mathematical model that describes the thermal process in the PCM is presented and differs from the analysis of conventional flat plate solar collectors making use of the lumped capacitance method which neglects spatial variations. The proposed model is calibrated favorably with a more detailed mathematical model that uses finite differences and considers temporal and spatial variations. Results for the collectors' thermal performance are presented along with the effects of the composition of the PCM. The thermal performance of an absorption machine coupled to an array of the proposed PCM solar collectors was investigated for nominal cooling capacities of 10.5, 14, and 17.5 kW. Computer simulations were conducted in which the heat and mass balances are applied on each component of the system, including the solar collectors, the air-cooled condenser, and the air-cooled absorber. Favorable comparisons are made with an absorption air conditioning system that uses a cooling tower with conventional flat plate collectors instead of air-cooled and PCM components. Useful information about physical dimensions of collectors, number of collectors needed, and efficiency of the overall system is presented.

---

\* Corresponding author. Present Address: Department of Mechanical Engineering, Santa Clara University, 500 El Camino Real, Santa Clara, CA, 95051. E-mail: [jgonzalezcruz@scu.edu](mailto:jgonzalezcruz@scu.edu)

## **NOMENCLATURE**

A:	area ( $\text{m}^2$ )
AHU:	air handling unit
c:	specific heat ( $\text{J/kg } ^\circ\text{K}$ )
E:	enthalpy (W)
$h_w$ :	heat transfer coefficient ( $\text{W/m}^2\text{-K}$ )
k:	thermal conductivity ( $\text{W/m-}^\circ\text{C}$ )
l:	tube longitude (m)
L:	latent heat ( $\text{J/kg}$ )
m:	mass (kg)
n:	time step
q:	heat flux received from the absorber ( $\text{W/m}^2$ )
$q_t$ :	top losses due convection and radiation ( $\text{W/m}^2$ )
R:	tube radius (m), thermal resistance ( $^\circ\text{K m}^2/\text{W}$ )
S:	absorbed solar radiation ( $\text{W/m}^2$ )
T:	temperature ( $^\circ\text{C}$ )
t:	time (s)
$U_T$ :	top loss coefficient from the absorber plate to ambient ( $\text{W/m}^2\text{-}^\circ\text{C}$ )
v:	fluid velocity (m/s)
x:	distance (m)

### ***Subscripts***

a	ambient
b:	bottom losses
CONV:	convective
i	inside
IN	inlet
INS	insulation
j:	node number
M:	melting
O	outside

OUT outlet

PCM: Phase Change Material

p: absorber plate

s: lateral area

### *Greek Symbols*

$\Delta$ : increase or decrease, insulation thickness (m)

$\rho$ : density ( $\text{kg/m}^3$ )

$\delta$ : plate thickness (m)

## INTRODUCTION

The use of solar driven absorption machines has been suggested during the past few years to offset the energy consumption in the Caribbean for air conditioning applications. Hernández et al. [1] presented a parametric study suggesting design parameters for solar driven closed absorption systems larger than 35kW in this region, providing information about the required collectors' area and size of the thermal storage tank as function of the cooling load. Meza et al. [2] presented experimental results for a 35kW closed absorption system in Puerto Rico demonstrating its operational feasibility. The system designed and investigated by Meza and co-workers, included a 35kW closed absorption machine driven by an array of 66 flat plate collectors of 1.71 m<sup>2</sup> frontal area each. A hot water storage tank to offset low radiation times, a gas boiler as backup system, and a cooling tower to remove the heat from the absorber and condenser of the absorption machine, complemented that system.

The largest market in the Caribbean for air conditioning systems is in the residential and light commercial sectors. The typical cooling load in these buildings ranges between 10.5 and 35 kW. Therefore, if solar driven absorption machines will be used to satisfy cooling needs in the residential and commercial sectors across the Caribbean, compact systems must be designed that eliminate the use of cooling towers and possibly of the thermal storage tank. Recently we proposed a compact absorption machine that somehow addresses this need of downsizing solar absorption machines [3]. The system proposed in that work is an air-cooled closed absorption machine where the water cooling is replaced by air cooling through the use of compact fans, for both the condenser and the absorber. We concluded in that work that the penalty for using air cooling is minimum if extremely compact and efficient heat exchangers are used. The proposed machine was suggested for 10.5, 14.0, and 17.5 kW cooling loads.

We now suggest in this work a mechanism to eliminate the use of storage tanks. We propose a flat plate solar collector that incorporates a phase change material (PCM) as a mechanism for thermal storage. We suggest here an analysis for the proposed PCM-solar collector and investigate its thermal performance and technical feasibility. The proposed method of analysis is the lumped capacitance method. The thermal performance of an air-cooled closed absorption machine driven by an array of the proposed PCM collectors is then investigated in detail. A

computer program is used to simulate the behavior of the PCM through the different working conditions as well as with the absorption cycle.

Figure 1 shows a typical solar absorption system with a cooling tower and a storage tank while Figure 2 shows the proposed air-cooled solar absorption system which does not make use of a cooling tower nor of a thermal storage tank using instead the proposed PCM-solar collectors and fans. It can be noted the simplification of the proposed system.

### **THE PCM-SOLAR COLLECTOR**

In this work the PCM-solar collector considered is conformed by a group of tubes immersed inside the PCM. The PCM is confined in separated and insulated rectangular containers so the PCM corresponding to a container as shown in Figure 3. No similar characteristics for a solar collector have been taken into account in the previous works reported in PCM collectors. Bansal et al. [4] and Rabin et al. [5] considered an arrangement of tubes over the PCM. Sokolov and Keizman [6] considered a PCM confined between two concentric tubes (solar pipe).

A lumped approach was used to investigate the PCM-solar collector along with the assumptions listed below in order to simplify the solution.

- Phase transition occurs at a single fixed temperature.
- Heat transfer inside the PCM Matrix is restricted to the conduction mode.
- No density change occurs while phase of PCM is changing.
- Physical properties are temperature independent.
- The local interface is assumed planar and sharp (a surface separating the phases), at the phase-change temperature.
- Surface tension and curvature effects at the interface are assumed insignificant.

For the solution of the phase change problem, the basic assumption is that the sensible heat is negligible compared to the latent heat (Stefan number is assumed zero), and consequently all the heat must be used to drive the phase-change [7]. Figure 4 shows the characteristics of the PCM element used in the analysis.

The lumped approach is compared with a method in which the energy equation is discretized by finite differences and that considers spatial and temporal variations. The method is commonly referred as the “enthalpy method” [7], and the results are shown later.

## **THE PARAFFIN-GRAPHITE COMPOSITE**

The composite considered in this work is the one proposed by Py et al. [8], which has a high thermal conductivity and a stable thermal power, as reported by Py et al. [8]. The composite is formed of two components: paraffin as the PCM and compressed expanded natural graphite (CENG). To conform the composite, graphite powders are poured into a mold of aluminum and then pressed to obtain the porous graphite matrix with the desired bulk density [8]. Then the matrix is soaked into melted paraffin and regularly weighted until maximum load is reached. In terms of capacity, and depending on bulk graphite density, the CENG/paraffin composites present a weight percentage ranging from 65% to 95% [8]. This is the range used in this work. Figure 5 shows the maximum paraffin weight loading versus bulk graphite matrix density, considering the loaded total porosity.

An important fact for the paraffin-graphite composite is that the heat storage capacity decreases with the increase of the CENG matrix density. This can be seen also in Figure 5, where the thermal storage capacity ratio is plotted versus the CENG matrix density. The thermal storage capacity ratio is the ratio of the effective thermal storage value to those obtained without CENG [8].

Table 1 shows the properties of the paraffin considered in this work.

## **THERMAL ANALYSIS FOR THE PCM**

Energy and mass balances were carried out for the PCM using the lumped capacitance method and the resulting equations are presented. For the absorber plate heat flux by conduction is considered as the heat transport mechanism to the PCM. The expression for the heat conduction through the absorber plate is:

$$S - U_T(T_p - T_a) - \frac{k}{\delta}(T_p - \bar{T}_{PCM}) = 0 \quad (1)$$

The above expression is solved at each time interval for the plate temperature using the secant method simultaneously with the PCM temperature whose solution is described below. The value of  $U_T$  is found using the relationship suggested by Duffie and Beckman [10] for mean plate temperatures between ambient and 200 °C to within  $\pm 0.3 \text{ W/m}^2\text{°C}$ :

$$U_T = \left\{ \frac{N}{\frac{C}{T_p} \left[ \frac{T_p - T_a}{N + f} \right]^e} + \frac{1}{h_w} \right\}^{-1} + \frac{\sigma(T_p + T_a)(T_p^2 + T_a^2)}{(\epsilon_p + 0.00591Nh_w)^{-1} + \frac{2N + f - 1 + 0.133\epsilon_p}{\epsilon_g} - N} \quad (2)$$

where:

N: number of glass covers

f:  $(1 + 0.089h_w - 0.1166h_w\epsilon_p)(1 + 0.07866N)$

C:  $520(1 - 0.000051\beta^2)$  for  $0^\circ < \beta < 70^\circ$

e:  $0.43(1 - 100/T_p)$

$\beta$ : collector tilt (degrees); ( $20^\circ$  in this work)

$\epsilon_g$ : emittance of glass; (0.9 in this work)

$\epsilon_p$ : emittance of plate; (0.09 in this work)

For the analysis of the PCM during **sensible heating** all the mass of the PCM is considered at the same temperature and energy is balanced in the entire control volume. Note that at this stage no melting of the PCM or fluid flow through the tubes is considered. The energy balance for this case is:

$$\left( \frac{mc}{A} \right)_{PCM} \frac{dT_{PCM}}{dt} = S - U_T(T_p - T_a) - \left( \frac{k}{\Delta} \right)_{INS}(T_{PCM} - T_a) \quad (3)$$

A melting stage for the PCM can be considered with no fluid flow through the tubes. During this stage the liquid and the solid phases are considered both to be at the melting temperature and the

interface is considered planar. The heat losses are accounted for in the energy balance at the top and bottom as well as the energy flux coming from the absorber. At this stage the position of the interface into the PCM is an important parameter and is represented by  $x(t)$ . The energy balance equation during melting is:

$$(L\rho)_{PCM} \frac{dx}{dt} = S - U_T(T_P - T_a) - \left(\frac{k}{\Delta}\right)_{INS} (T_M - T_a) \quad (4)$$

A **simultaneous stage** can be simulated in which solar radiation is available and a fluid is circulating through the solar collector while energy is being removed and added **simultaneously** from and to the PCM. Equation (5) below is used for the final temperature of the PCM, which results from the application of an energy balance (only when temperature of the PCM is above the melting temperature).

$$\frac{dT_{PCM}}{dt} = \left(\frac{A}{mc}\right)_{PCM} \left\{ S - U_T(T_P - T_a) - \left(\frac{k}{\Delta}\right)_{INS} (T_{PCM} - T_a) \right\} - \frac{1}{(mc)_{PCM}} q_{CONV} \quad (5)$$

For this **simultaneous** stage when the temperature reaches the melting temperature and solidification begins around the collector tube, a radial configuration is considered similar to that shown in Figure 6, and Equation (6) is used for the position of the interface at each time interval.

$$\frac{dR}{dt} = \left(\frac{1}{2\pi(L\rho l)_{PCM}}\right) \frac{1}{r} \left\{ q_{CONV} + A \left[ U_T(T_P - T_a) + \left(\frac{k}{\Delta}\right)_{INS} (T_{PCM} - T_a) - S \right] \right\} \quad (6)$$

The absorbed solar radiation ( $S$ ) is taken into account, and all of the heat must be used to drive the phase-change process, maintaining a radial configuration for the interface position, and to add heat to the fluid simultaneously. Therefore, this considers that energy is being removed by convection for the fluid inside the tubes.

The set of Equations (3) to (6) were solved simultaneously by the Runge Kutta 4<sup>th</sup> Order numerical method considering that the initial thermal state of the PCM was in equilibrium with the ambient.

For the **melting** stage (charging) all the PCM is considered to be solidified, solar energy is transmitted to the composite by the absorbing plate, and no energy is removed inside the tubes, so energy is transmitted from the most upper side to the bottom. For this case a flat interface can be assumed. During the **simultaneous** stage all the composite is considered to be melted, heat is being removed inside the tubes and solar radiation is available. Therefore solidification is expected to occur around the tubes and a radial configuration can be assumed for the interface. There is no conflict because charging and simultaneous stages are assumed to take place at different times.

The output fluid temperature and the energy removed from the solar collectors by forced convection is calculated under the assumption of a constant PCM temperature along the collector tubes. For the collector's outlet fluid temperature a differential element is considered inside the tube. The integration along the axial direction of the collector tube gives the following expression:

$$T_{OUT}(z) = T_i + e^{-\gamma z} [T_{IN} - T_i] \quad (7)$$

where

$$\gamma = \frac{2h}{R_{IN} \nu \rho c}$$

The expression for the convective heat flux is given by [11]:

$$q_{CONV} = A_s h \frac{(T_i - T_{OUT}) - (T_i - T_{IN})}{\ln\left(\frac{T_i - T_{OUT}}{T_i - T_{IN}}\right)} \quad (8)$$

The inside wall temperature of the copper tube can be expressed as:

$$T_i = \frac{T_{PCM} + \beta T_{IN}}{1 + \beta} \quad (9)$$

And

$$\beta = A_s h \frac{\ln\left(\frac{R_o}{R_{IN}}\right)}{2\pi l K} \frac{e^{-\beta} - 1}{-\beta} \quad (10)$$

The Biot number used in this work represents the ratio of the convective effects to the spatial conduction and is an important parameter to observe when using the lumped capacitance method. Its value should be less than 0.1 for the lumped capacitance method to be valid [11]. It is defined as:

$$Bi = \frac{hL_c}{k} \quad (11)$$

Where  $L_c$  is the characteristic length (see Figure 6),  $h$  is the convection coefficient inside the tube and  $k$  is the conductivity of the composite.

## THE VALIDATION METHOD

The method used to validate the results obtained with the lumped capacitance method is referred as the Enthalpy Method [7]. The results obtained with the lumped capacitance method are compared with the results obtained with this enthalpy method. The enthalpy method is based on the conservation of energy expressed in terms of enthalpy and temperature. The energy conservation applied to a one-dimensional problem is expressed in the form:

$$\int_{t_n}^{t_{n+1}} \frac{\partial}{\partial t} \left( A \int_{x_{j-1/2}}^{x_{j+1/2}} E(x,t) dx \right) dt = - \int_{t_n}^{t_{n+1}} A \int_{x_{j-1/2}}^{x_{j+1/2}} q_x(x,t) dx dt \quad (12)$$

Here the enthalpy  $E$  is the sum of sensible and latent heat in the liquid. Proceeding with the discretization of the control volume in a finite number of nodes, a backward in time and central in space difference formulation is used. The following expressions are obtained for the enthalpy of each node:

$$E_j^{n+1} = E_j^n + \frac{\Delta t_n}{\Delta x_j} [q_{j-1/2}^n + q_{j+1/2}^n] \quad (13)$$

The heat flux between nodes is

$$q_{j-1/2}^n = -\frac{T_j^n - T_{j-1}^n}{R_{j-1/2}} \quad (14)$$

The temperature of the nodes is

$$\text{Solid}(E_j^n \leq 0) \dots T_j^n = T_m + \frac{E_j^n}{\rho c_s} \quad (15)$$

$$\text{Interface}(0 < E_j^n < \rho L) \dots T_j^n = T_m \quad (16)$$

$$\text{Liquid}(E_j^n \geq \rho L) \dots T_j^n = T_m + \frac{E_j^n - \rho L}{\rho c_L} \quad (17)$$

The total mass of the PCM was divided in five nodes and each node was differentiated at the center of each section. The first node is considered to be placed in the section under the absorber plate and the last node in the section immediately over the bottom insulation. Results obtained from the enthalpy method are presented in the next sections and are compared with those obtained with the lumped capacitance method.

## DESCRIPTION OF THE SIMULATION

The thermal performance of the PCM was investigated both individually and coupled to an air-cooled absorption cycle. In the simulation, the tilted radiation is estimated hourly and monthly for a location in Puerto Rico using the Perez model [12]. The southern city of Ponce (latitude 18.2°, longitude 67.1°) and the month of July were considered for the analysis. The simulation scheme for the air-cooled absorption machine is a modified version of the analysis presented by Alva and González [3]. That simulation is for a coupled system consisting of solar collectors, a non-stratified storage tank and a single effect air-cooled absorption machine. The refrigerant

considered is water and the absorbent is lithium bromide solution. A variable cooling load is fed into this program and the results for the hot water mass flow rate of the desorber of the air-cooled absorption machine were used as input to the PCM simulation program. A variable cooling load for a typical building application is considered for the hours from 8:00 to 17:00 and is shown in Figure 7 for 10.5, 14 and 17.5 kW of peak cooling loads. The roof areas considered for each nominal load were 100, 158, and 219 m<sup>2</sup>, respectively. Available data for the city of Ponce for the temperature, the horizontal total radiation, and the relative humidity are used [13]. An important fact is that during off sunshine hours an insulating cover is considered over the collector glazing to prevent energy losses. Results are presented in the next section.

## RESULTS

To take advantage of the highest conductivity the percentage by weight of the paraffin considered in this work was 65%. Data of the composite's conductivity for materials with a paraffin content of less than 65% are not available [8] and are not considered in this work. Figure 8 shows the variation of the thermal conductivity of the composite material considered with temperature.

A range between 0.06 and 0.04 meters of PCM width was found to be acceptable to avoid excessive melting for given mass flow rates while maintaining a uniform melting as indicated by the small values of the Biot number. The corresponding mass flow rates inside the tube that can be allowed for this range of PCM material was between 0.001 and 0.002 kg/s per element. Higher values of mass flow rates may induce fast solidification of the PCM.

Figure 9 shows the minimum 65%-paraffin composite area, corresponding to a maximum solidification permitted of approximately 80%, with respect to the maximum mass flow rate per tube that can be supported under the lumped capacitance method. The maximum solidification is considered when the interface diameter equals the depth of the composite. The constant flow rate inlet temperatures considered were 60°C, 65 °C, 70 °C, 75 °C, and 80°C. Areas lower than the values showed may result in PCM solidification rates in excess of 80%, and consequently the PCM-collector may not work appropriately. Areas larger than the presented values will make the collector less efficient because it will require more energy to melt completely. It can be

noted that the composite material has a linear behavior with respect to the mass flow rate, with zero intercept.

The value for the minimum composite area corresponding to an assumed mass flow rate per tube and an assumed flow rate inlet temperature is a design parameter to be considered when sizing the area of PCM collectors needed for a given application. In actual working conditions, the mass flow rate and the collector input temperature may be different than that assumed values to find the minimum composite area.

The width and length of a composite element are shown in Figure 10 with respect to the mass flow rate per tube when a minimum composite area and a maximum solidification of 80 % is considered. As can be seen, as the mass flow rate per tube increases the width of the element decreases, and the length increases.

The area of the composite is the product of the composite's width and the composite's length. Since the width is taken as the maximum permitted, then the length results in the minimum, as can be observed in Figure 10. Figure 11 shows the total collector area and the collector efficiency vs. the composite's width, for an element with a mass flow rate of 0.00142 kg/s. This mass flow rate was selected arbitrarily in order to work with a small collector area. In the case shown in Figure 11, for a composite's width in the range of 0.049 and 0.056 m the maximum collector efficiency and the minimum total collector area is reached. The value of 0.056 m for the width of the composite was used to simulate the solar air cooling system for cooling loads of 10.5, 14, and 17.5 kW.

The warming of the PCM from ambient temperature to melting temperature is shown in Figure 12. The location of Ponce, Puerto Rico, and month of July were considered for this simulation. It can be observed that it takes less than four hours for the 65%-paraffin composite to reach the paraffin melting temperature of 89 °C. Warming of the PCM was simulated for the hours from 7:00 to 11:00, for which the corresponding average horizontal total radiation was 1687.9 kJ/h m<sup>2</sup>.

In Figure 12, the increase in the slope of the curve after 1 hour is because there is a higher increment in temperature due to the higher solar radiation available at this moment.

Melting of the paraffin was considered to begin at 11:00 immediately after warming and was simulated for the same location. The differences in slopes are due to the varying solar radiation that reaches a maximum at 12:00 and then decreases. It is also shown in Figure 13 that melting of the 0.056 m in depth PCM material is reached after 4 hours, for an average horizontal total radiation of 2925.5 kJ/h m<sup>2</sup>.

From 18:00 to 6:00 hours the solar collector was considered to be covered by a 0.04 m insulation layer to prevent heat losses due to radiation and convection from the cover surface to the ambient. Without any insulation over the collector cover the energy losses could be too high inhibiting the operation of the collector due to melting.

The behavior of the PCM-solar collector is somehow different when the cooling load considered is variable. For this case, the load that must be supplied to the desorber of the air-cooled absorption machine changes with time in the same way the variable cooling load changes. Therefore a different desorber load distribution is obtained respect to the case when a constant cooling load is considered. Details of the PCM-solar collector's dimensions, mass flow rates and number of collectors for the cases of 10.5, 14, and 17.5 kW of dynamic cooling load are shown in Table 2.

Table 3 shows the results for an air-cooled absorber machine under variable cooling load and coupled to an array of conventional flat plate collectors. As can be seen the total collector area needed for the case of using PCM-solar collectors is higher than that for the case of using conventional flat plate collectors. The total PCM collector area is 4.7, 5.8 and 6.8 m<sup>2</sup> higher than the corresponding total area needed using conventional flat plate collectors for 10.5, 14 and 17.5 kW of cooling load, respectively.

The hourly solar fraction is shown in Figure 13 for a variable cooling load and a 65%-paraffin composite, and for working hours between 8:00 and 17:00. As can be observed, the solar

fraction is close to 100% except between 10:00 and 15:00 hours where it is variable, and reaches values as low as 70%. The variation of the solar fraction is because the inlet temperature needed to heat the generator of the absorption machine changes with time reaching temperatures higher than the outlet collector temperature. A similar behavior was found for the cases of 10.5, 14, and 17.5 kW of cooling load.

The daily collector efficiency is calculated at the end of the working hours (8:00 to 17:00 in this work), and for the case of variable cooling load was found to be 0.43. An hourly PCM-solar collector efficiency was difficult to calculate because the absorbed solar radiation is not removed directly for the fluid passing through the collector but is stored in the PCM. The fluid passing through the collector is removing energy from the PCM. Therefore the energy removed by the fluid could be larger than the solar radiation available and absorbed by the collector at that particular hour.

Figure 14 shows the daily average solar fraction for the cases of systems with PCM-collectors and an air-cooled absorption machine, with flat plate collectors and air-cooled absorption machine, and with a water-cooled absorption machine with flat plate collectors all under variable cooling load. As can be seen the PCM-collectors system gives a higher solar fraction than the other cases considered. With respect to the flat plate collectors coupled to an air-cooled machine the difference is around 5%. It should be emphasized that when using PCM-collectors the storage tank is not needed.

Finally, a schematic design of the proposed PCM solar collector is shown in Figure 15. The depth is about 0.14 m. The weight of the composite in the collector is around 72 kg, considering 30 kg due to the collector then the total collector weight would be around 102 kg. Therefore precautions would have to be considered for roof installations.

A validation procedure for the lumped capacitance method was conducted by comparing the lumped capacitance method to the enthalpy method described above. To compare both methods simulations were conducted for a constant ambient temperature of 30.74 °C and a tilted solar irradiation of 526 W/m<sup>2</sup>. The dimensions of the PCM element considered are 0.056 m in width

and 3.583 m in length. In Figure 16 are presented the results for the warming process of the PCM from the ambient temperature to the PCM's melting temperature (89 °C) for both methods. Five nodes across the width of the PCM were considered for the case of the enthalpy method and the transient for each node is presented in Figure 16 as well. As can be observed the results from both methods are very similar. The PCM reaches the melting temperature in 196.3 minutes using the lumped capacitance method, and with the enthalpy method in 160.5 minutes. The time both methods take to reach complete melting from is shown in Figure 17 where the total solidified volume for both methods is presented. Here the lumped capacitance method predicts that the PCM will melt completely in 524.3 minutes, while the enthalpy method predicts it will occur in 512.5 minutes.

## CONCLUSIONS

Results for the PCM-solar collector proposed using a 65% paraffin-graphite composite are very encouraging and the feasibility of this kind of equipment is clear. Therefore, there is an apparent indication that conventional storage tanks may be replaced for the PCM integrated in the solar collector. The following specific conclusions can be drawn from this work,

- The paraffin-graphite composite with 65% of paraffin in weight was found to work best mainly because of the highest conductivity obtained.
- A minimum composite-element area was found for which a maximum solidification of approximately 80% was permitted to occur. This area depended strongly on the element mass flow rate and the collector input temperature and was an important parameter to size the collector's area necessary to be used in an air-cooling application.
- A maximum width of the PCM was found which provides the highest daily collector efficiency and the minimum total collector area.
- When the PCM was coupled to an air-cooled absorption machine, it was found that an element having width a of 0.056 m would work well for the application with peak cooling loads between 10.5 and 17.5 kW and using a 65%-paraffin composite. To find

the minimum composite-element area needed the element mass flow rate was 0.00142 kg/s and the input collector temperature was 80 °C.

- For the cases of 10.5, 14, and 17.5 kW of cooling load and climatic conditions prevailing in Puerto Rico, the needed PCM-collector area was found to be 4.7, 5.8 and 6.8 m<sup>2</sup> higher than the collector area needed when using conventional flat plate collectors and storage tank.
- The daily solar fraction for a system with PCM-solar collectors with an air-cooled machine was 5% higher than when using flat plate collectors coupled to an air-cooled absorption machine under variable cooling load using a storage tank.
- The lumped capacitance method was compared with a one-dimensional method that uses finite differences and the results for warming and melting of the PCM were very similar. Therefore, the results obtained using the lumped capacitance method are acceptable and representative of the phenomenon being simulated.

## REFERENCES

1. Hernández H., González J.E., and Khan A.Y., 1997, "A parametric Study of Solar Assisted Air Conditioning and Dehumidification Systems Operating in the Caribbean Region", Proceedings of the ASME Solar Energy Division, pp. 327-334.
2. Meza J.I., Khan A. Y., and González J. E., 1998, "Experimental Assessment of a Solar-assisted Air Conditioning System for Applications in the Caribbean", Proceedings of the ASME Solar Energy Division, pp. 149-154.
3. Alva L.H. and González J.E., 2002, "Simulation of an Air-cooled Solar-assisted Absorption Air Conditioning System", Journal of Solar Energy Engineering, vol. 124, pp. 276-282.
4. Bansal N.K. and Buddhi D., 1992, "Performance of a Cum Storage System", Journal of Solar Energy, vol. 48, pp. 185-194.
5. Rabin Y., Bar-Niv I., Korin E., and Mikic B., 1995, "Integrated Solar Collector Storage System Based on a Salt-hydrate Phase-change Material", Journal of Solar Energy, vol. 55, pp. 435-444.
6. Sokolov M. and Keizman Y., 1991, "Performance Indicators for Solar Pipes with Phase Change Storage", Journal of Solar Energy, vol. 47, pp. 339-346.
7. Alexiades V. and Solomon A. D., 1993, "Mathematical Modeling of Melting and Freezing Processes", Whashington; Hemisphere Publishing Corporation.
8. Py X., Olives R. and Mauran S., 2001, "Paraffin/porous-graphite-matrix Composite as a High and Constant Power Thermal Storage Material", International Journal of Heat and Mass Transfer, vol. 44, pp. 2727-2737.
9. Hoogendoorn C.J. and Bart G.C.J., 1992, "Performance and Modeling of Latent Heat Stores", Journal of Solar Energy, vol. 48, pp. 53-38.
10. Duffie J.A. and Beckman W. A., 1991, "Solar Engineering of Thermal Processes", New York; John Wiley & Sons, Inc.
11. Incropera F. P. and DeWitt D. P., 1996, "Fundamentals of Heat and Mass Transfer", New York; John Wiley & Sons.
12. Perez R., Seals R., Ineichen P., Stewart R. and Menicucci D., 1987, "A New simplified Version of the Perez Diffuse Irradiance Model for Tilted Surfaces", Journal of Solar Energy vol. 39, pp. 221-231.

13. Hernández H., 1997, “Analysis and Modeling of a Solar-Assisted Air Conditioning and Dehumidification System for Applications in Puerto Rico”, M.S. Thesis; University of Puerto Rico, Mayagüez, P.R., USA.

Table 1: Paraffin Properties (Data from Hoogendoorn and Bart [9]).

Melting Temp.	Density	Latent Heat	Spec. Heat	Conductivity
(°C)	(kg/m <sup>3</sup> )	(kJ/kg)	(J/kg °C)	(W/m °C)
89	900	179	1770	0.2

Table 2: Results for the Case of an Air-cooled Absorption Machine with PCM-Solar Collectors.

Load (kW)	m.f.r. (kg/s)	C. Length (m)	width (m)	depth (m)	Coll.Area (m <sup>2</sup> )	Collector Number	Total Coll. Area (m <sup>2</sup> )
10.5	0.3181	3.583	0.056	0.056	1.605	30	48.2
14	0.4658	3.583	0.056	0.056	1.605	40	64.2
17.5	0.5566	3.583	0.056	0.056	1.605	49	78.7

Table 3: Results for the Case of an Air-cooled Absorber Machine with Conventional Flat Plate Collectors.

Load (kW)	m.f.r. (kg/s)	C. Length (m)	Coll.Area (m <sup>2</sup> )	Collector Number	Total Coll. Area (m <sup>2</sup> )
10.5	0.29	1.93	1.67	26	43.42
14	0.43	1.93	1.67	35	58.45
17.5	0.52	1.93	1.67	43	71.81

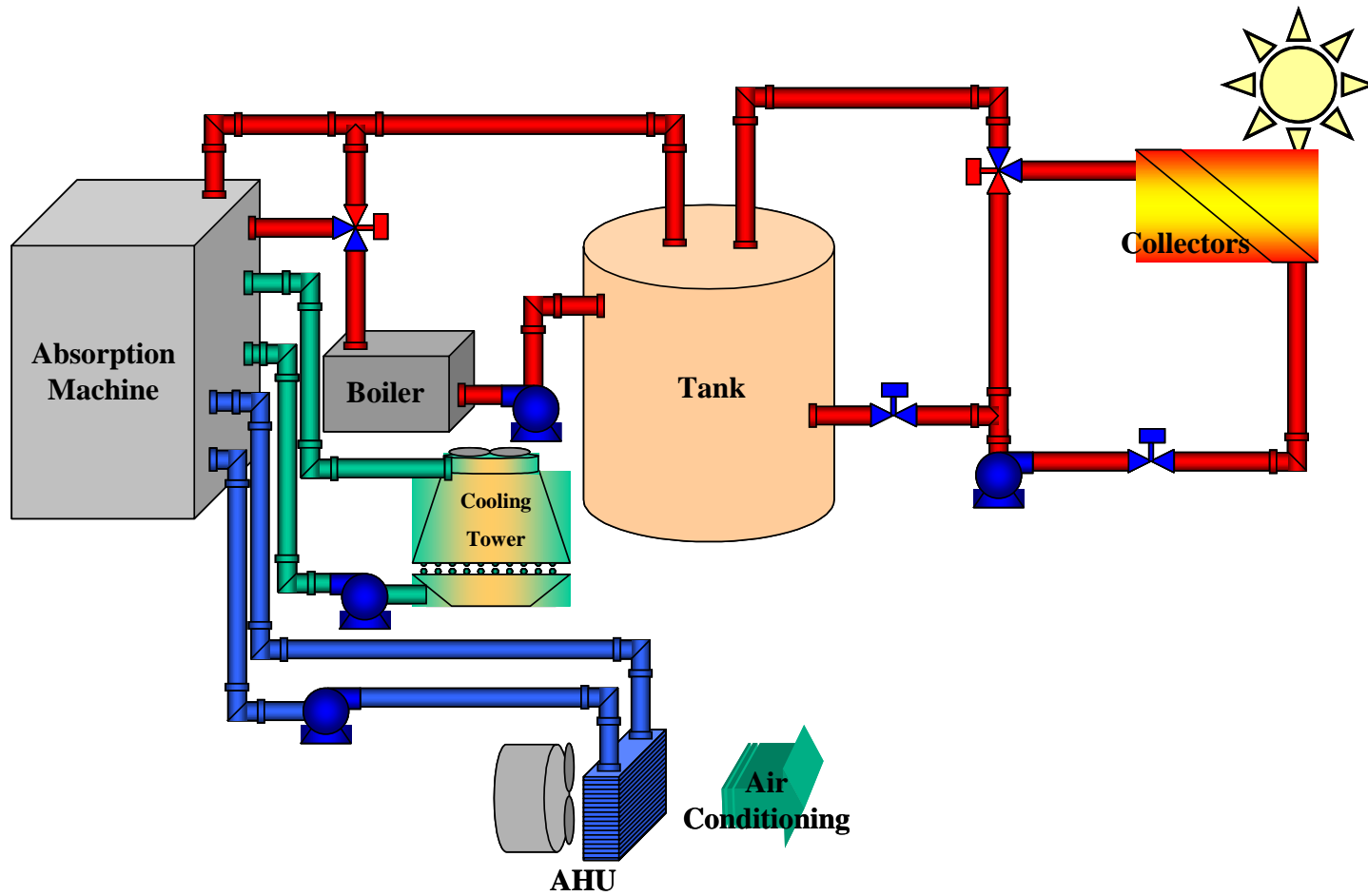


Figure 1: Solar Absorption System with Cooling Tower.

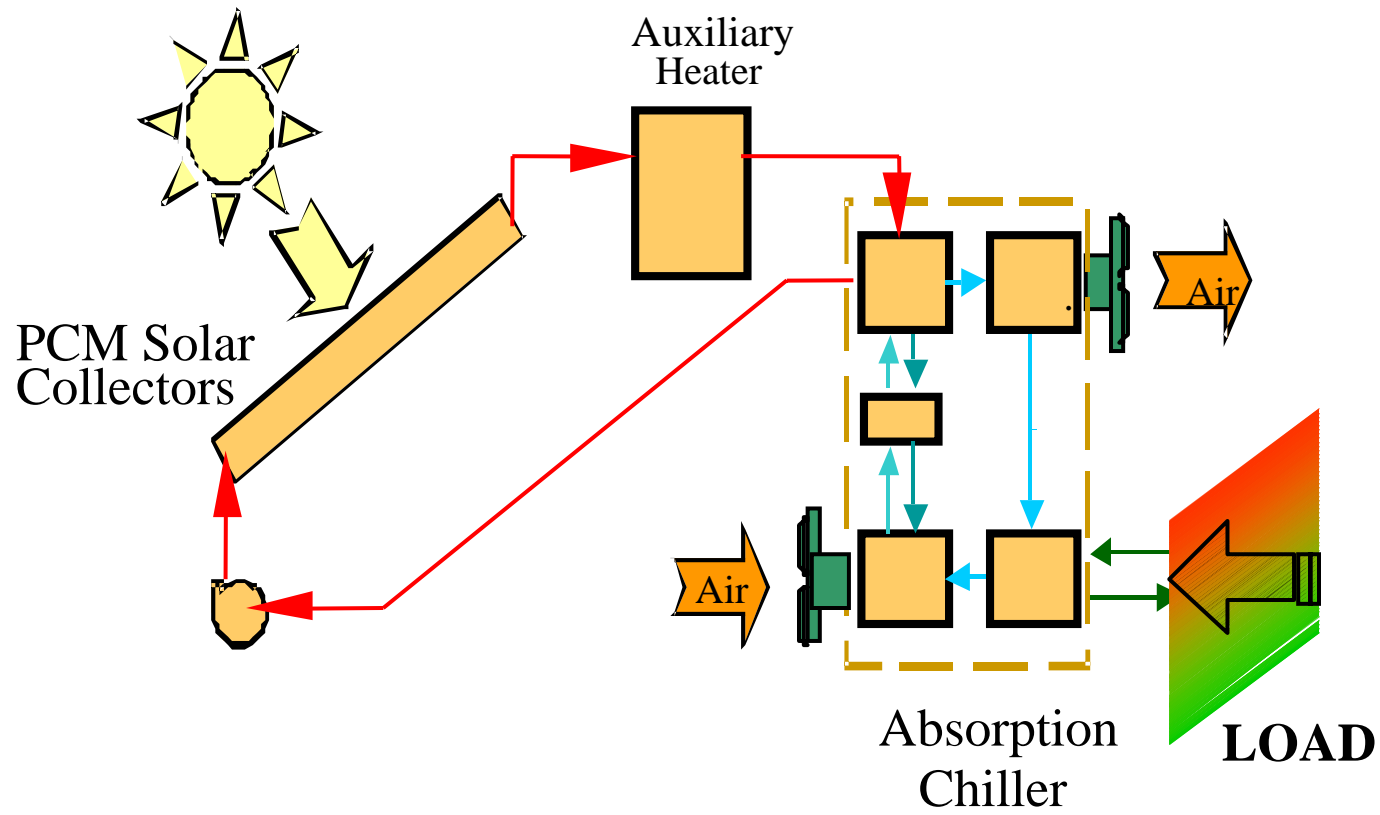


Figure 2: Air-Cooled Solar Absorption System with PCM

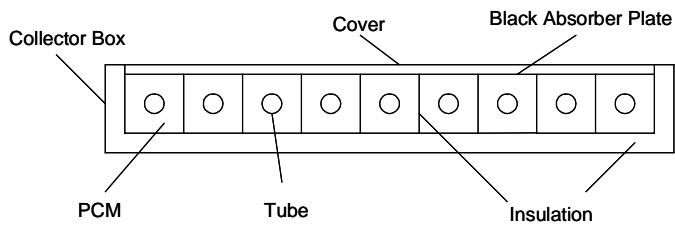


Figure 3: Schematic of the PCM Solar Collector.

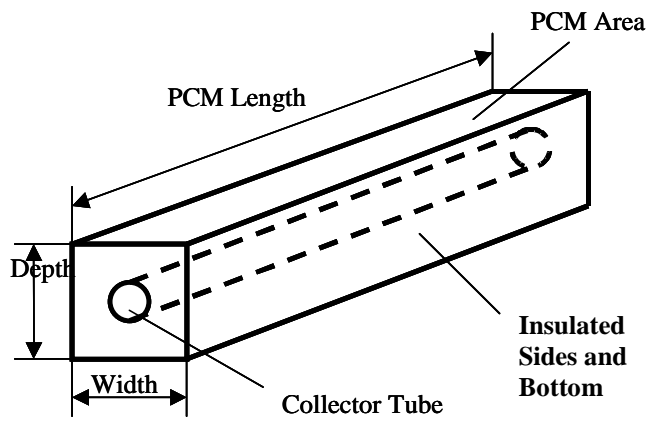


Figure 4: PCM Element Configuration.

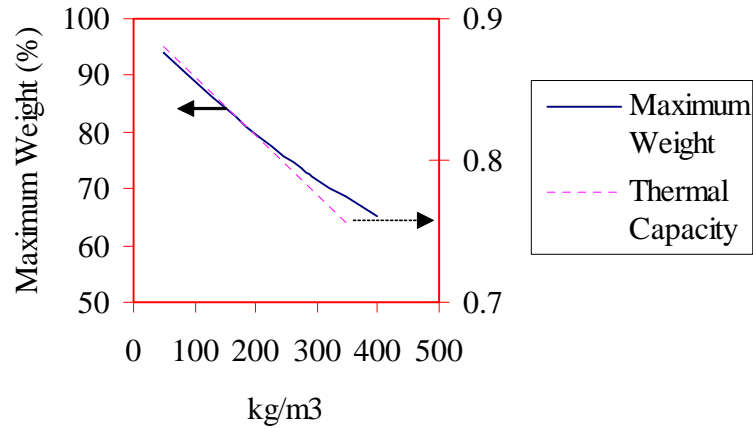


Figure 5: Maximum Paraffin Weight in Percentage and Reduced Storage Thermal Capacity vs. Graphite Matrix Density (Loaded Total Porosity) [8].

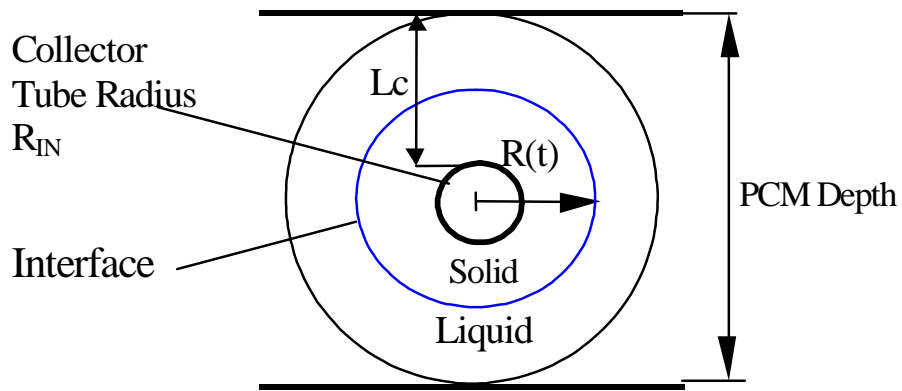


Figure 6: Schematic Representation of the PCM for the Simultaneous Stage.

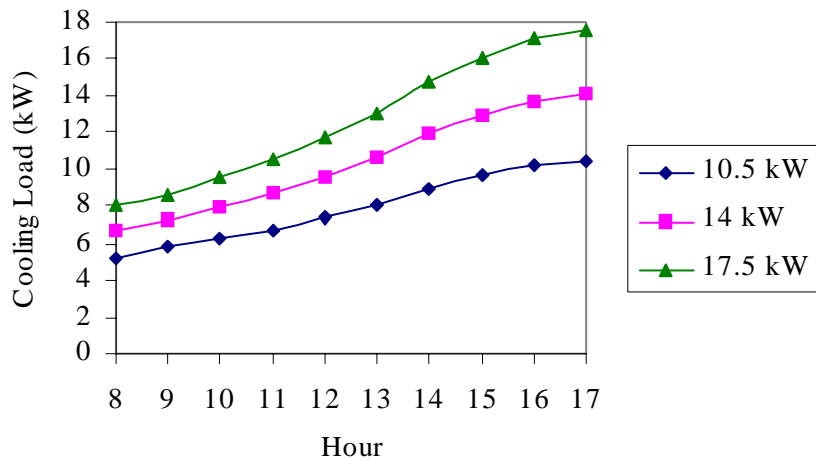


Figure 7: Variable Cooling Load used in the Simulations.

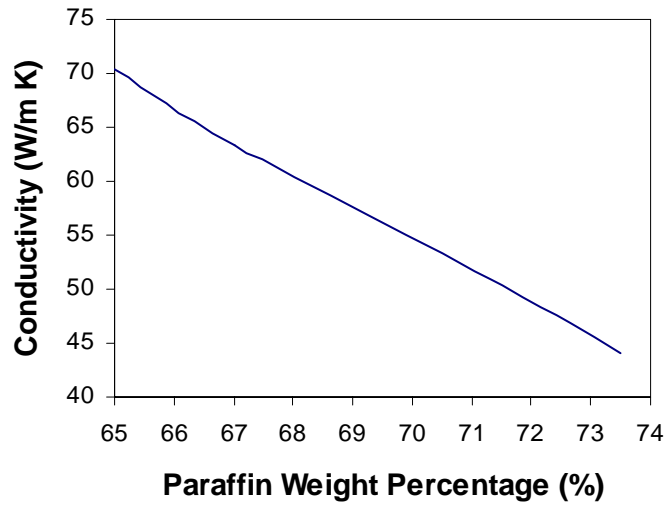


Figure 8: Composite Conductivity vs. Paraffin Weight Percentage.

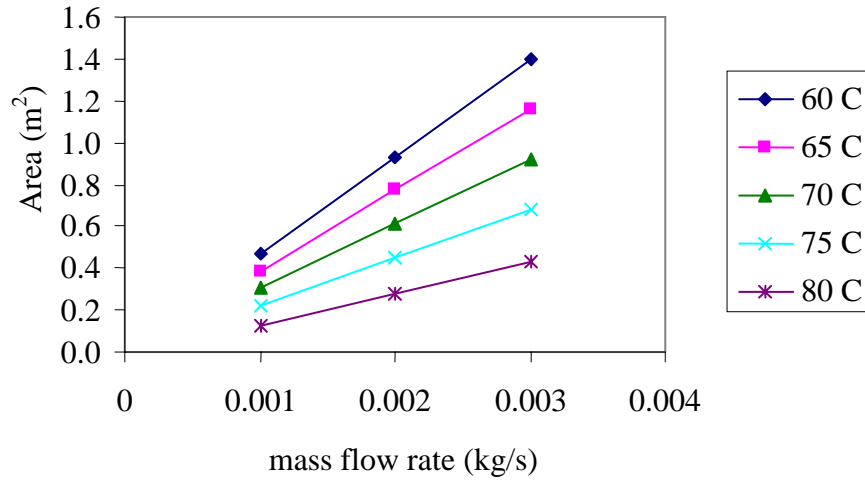


Figure 9: Minimum Composite Area vs. Maximum Mass Flow Rate for Different Inlet Temperatures.

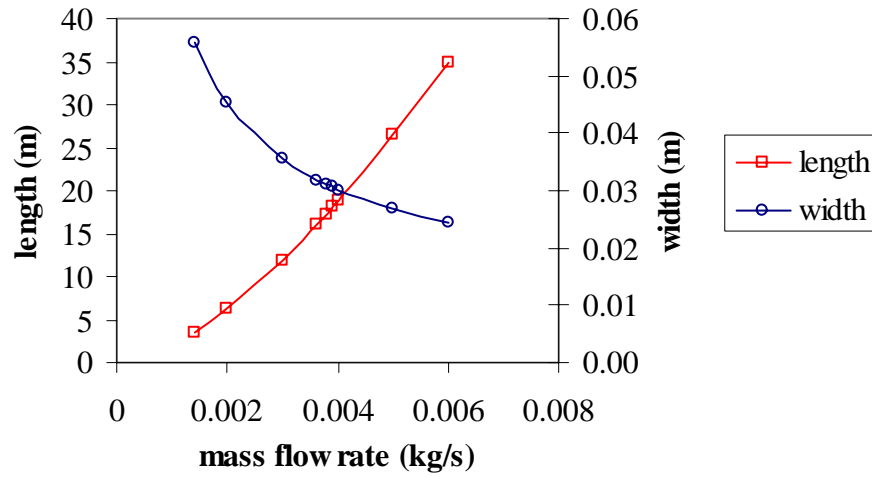


Figure 10: Width and Length of the Composite Material.

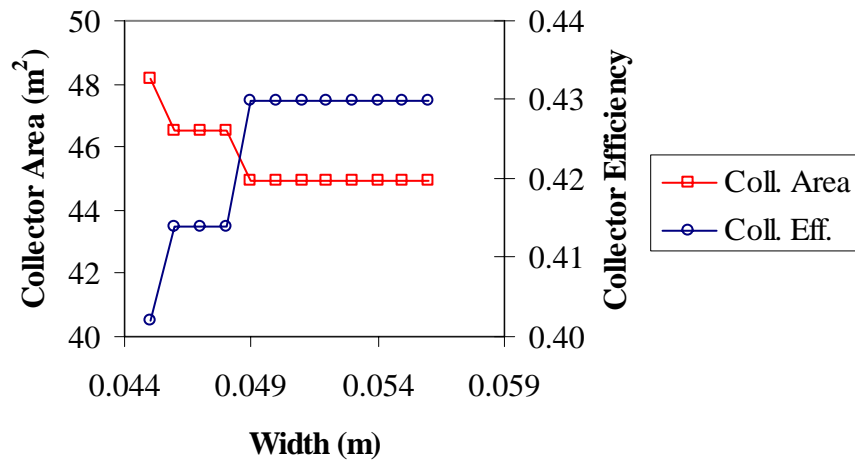


Figure 11: Collector Area and Collector Efficiency vs. PCM's Width (For a mass flow rate equal to 0.00142 Kg/s).

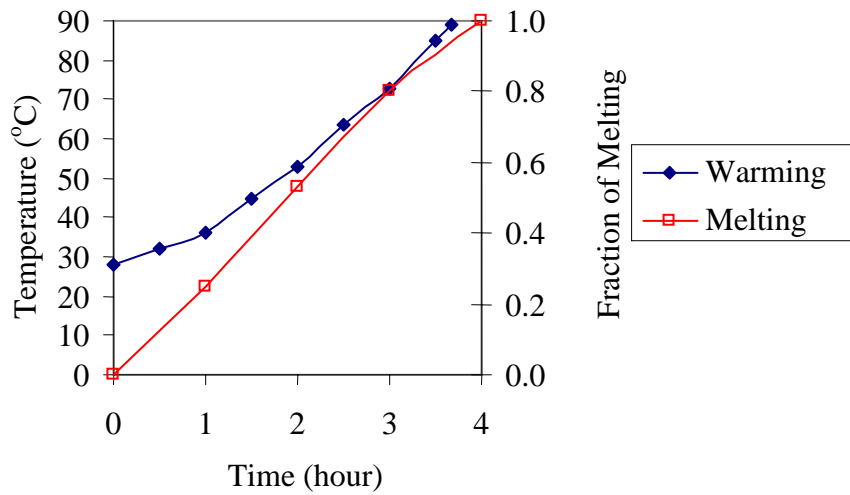


Figure 12: Warming and Fraction of Melting of the 65%-Paraffin Composite.

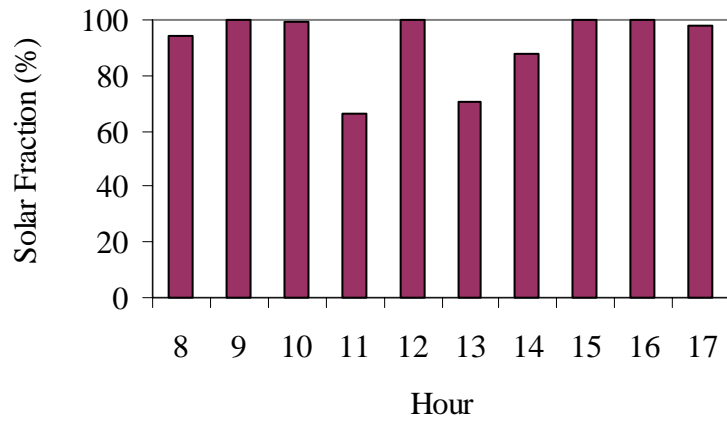


Figure 13: Hourly Solar Fraction for a PCM-collector and air cooled solar absorption system under Dynamic Cooling Load.

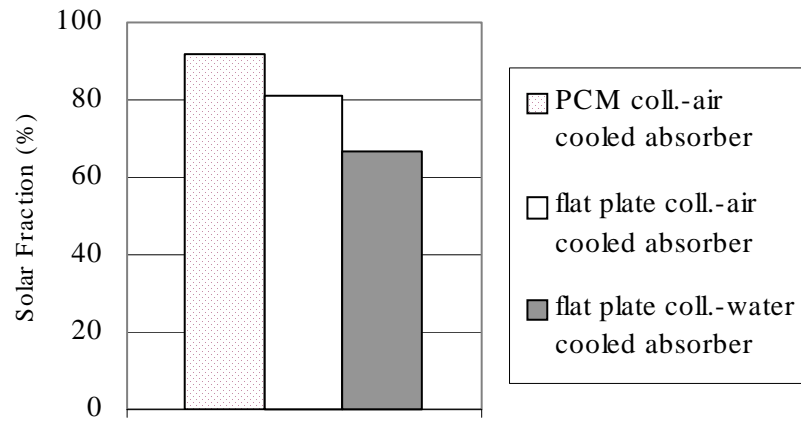


Figure 14: Daily Average Solar Fraction for Month July and Location Ponce, P.R..

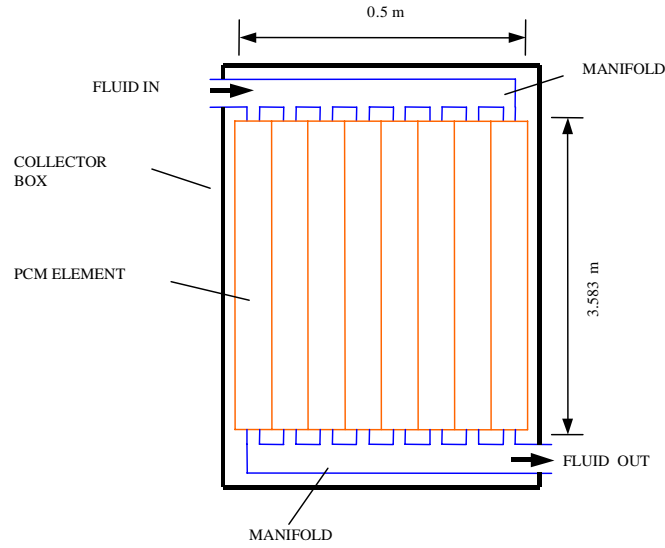


Figure 15: Proposed PCM Solar Collector.

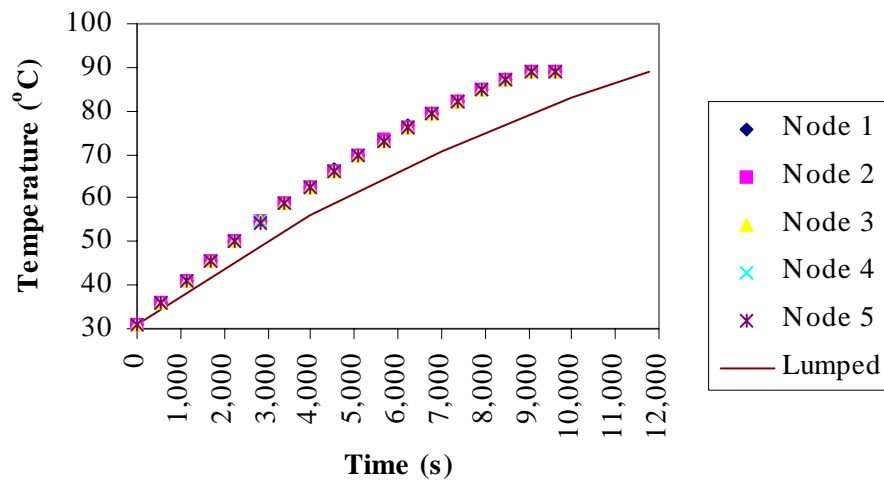


Figure 16: Comparison of the Warming Process of the PCM for Results Given by the Lumped Capacitance Method and the Enthalpy Method Using Five Nodes.

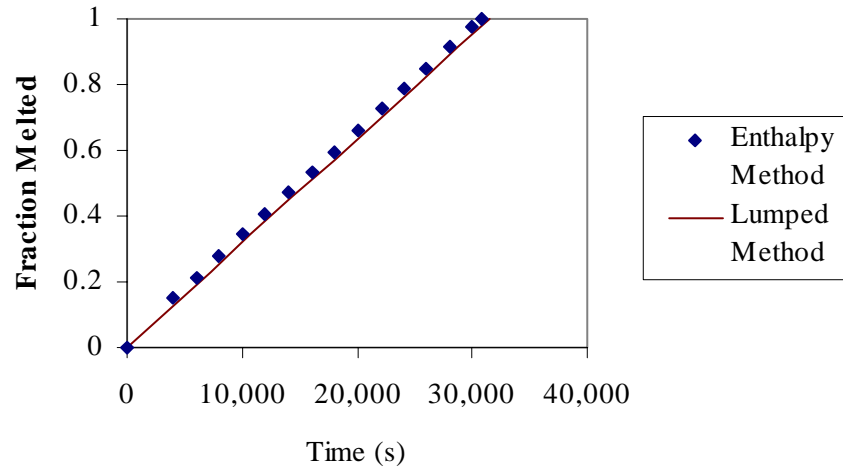


Figure 17: Comparison of the Total Volume Melted for Results given by the Lumped Capacitance Method and the Enthalpy Method.